

The effects of saturation and velocity selective population in two-step $6S_{1/2} \rightarrow 6P_{3/2} \rightarrow 6D_{5/2}$ laser excitation in cesium

Vlasta Horvatic^{b,*}, Tiffany L. Correll^a, Nicolás Omenetto^a,
Cedomil Vadla^b, James D. Winefordner^a

^a Department of Chemistry, University of Florida, Gainesville, FL 32611, USA

^b Institute of Physics, 10000 Zagreb, Croatia

Received 17 July 2006; accepted 12 October 2006

Abstract

Excited states population distributions created by two-step $6S_{1/2} \rightarrow 6P_{3/2} \rightarrow 6D_{5/2}$ laser excitation in room temperature cesium vapor were quantitatively analyzed applying absorption and saturation spectroscopy. A simple method for the determination of the excited state population in a single excitation step that is based on the measurements of the saturated and unsaturated absorption coefficients was proposed and tested. It was shown that only $\approx 2\%$ of the ground state population could be transferred to the first excited state by pumping the Doppler broadened line with a single-mode narrow-line laser. With complete saturation of the second excitation step, the population amounting to only $\approx 1\%$ of the ground state can be eventually created in the $6D_{5/2}$ state. The fluorescence intensity emerging at $7P_{3/2} \rightarrow 6S_{1/2}$ transition, subsequent to the radiative decay of $6D_{5/2}$ population to the $7P_{3/2}$ state, was used to assess the efficiency of the population transfer in the chosen two-step excitation scheme. The limitations imposed on the sensitivity of such resonance fluorescence detector caused by velocity-selective excitation in the first excitation step were pointed out and the way to overcome this obstacle is proposed.

© 2006 Elsevier B.V. All rights reserved.

Keywords: Saturation; Velocity selectivity; Two-step excitation; Doppler-free spectra; Cesium

1. Introduction

Availability of single-mode tunable lasers having line widths much smaller than the thermal Doppler width of the spectral lines of atoms in a vapor, gave rise to many investigations that require velocity-selective excitation. In the case of predominant inhomogeneous e.g. Doppler broadening, atoms do not absorb monochromatic radiation with equal probability. Rather, the probability of absorption depends upon each atom's velocity. Only those atoms, which are Doppler-shifted into resonance with the radiation, can interact with the field, and a narrow velocity group can be selected, resulting with a population of excited-state atoms that all have the same velocity component along the pump-laser propagation direction. Velocity-selective pumping has important applications in saturation spectroscopy

[1,2], line shape studies [3,4], laser cooling of atoms [5], and the study of velocity-changing collisions [6].

Some optical techniques, in addition to velocity-selective excitation, require also creation of high populations in the excited states. Examples are single-point photon detectors, such as resonance fluorescence/ionization detectors (RFDs/RIDs), and resonance fluorescence/ionization imaging detectors (RFIDs/RIIDs) [7–18]. To maintain high spectral resolution and minimize the effects of radiation trapping these devices utilize narrow-band laser excitation in Doppler broadened medium, which leads to velocity-selective pumping. In order to enable quality signal conversion in a particular excitation/ionization scheme these detectors also require production of high excited state populations. Another research area where the combined need of applying velocity selectivity in excitation and obtaining high excited atomic populations is often encountered is in the field of collisional excitation energy transfer investigations. Measurement of the cross sections for the particular collisional transfer process requires the determination of the atom number densities in the states involved

* Corresponding author. Tel.: + 385 1 469 8861; fax: +385 1 469 8889.
E-mail address: blecic@ifs.hr (V. Horvatic).

in the reaction. Fluorescence, absorption or thermionic diode signals are usually used as a measure of the excited population created [19–26]. If, for instance, measurements are performed in a pure atomic vapor excited at $|1\rangle \rightarrow |2\rangle$ transition with single-mode laser, and the population of the state $|2\rangle$ is measured by monitoring the fluorescence at $|2\rangle \rightarrow |1\rangle$ transition, the high population in the state $|2\rangle$ is favorable to produce fluorescence signals of adequate quality. However, to avoid trapping of fluorescence radiation, the population the initial state $|1\rangle$ should be kept low, resulting in turn with pumping in the Doppler broadened $|1\rangle \rightarrow |2\rangle$ transition, i.e. with velocity-selective excitation.

Recently, the atomic vapor fluorescence detector using Cs has been reported [13] and analyzed from the aspect of simultaneous improvement of the efficiency of the chosen two-step excitation scheme and minimization the occurrence of radiation trapping and image distortion [27]. In this device, the cesium $6D_{5/2}$ population is created with two-step $6S_{1/2} \rightarrow 6P_{3/2} \rightarrow 6D_{5/2}$ laser excitation. The $6D_{5/2}$ population radiatively decays to the $7P_{3/2}$ state eventually resulting with fluorescence at $7P_{3/2} \rightarrow 6S_{1/2}$ transition. This wavelength-shifted fluorescence serves as the analytical signal indicating that the initial absorption event occurred. The positive influence of this selective excitation on the spectral resolution of atomic vapor filters and photon detectors has been well characterized [16,17]. However, velocity-selective excitation also imposes significant limitations on the efficiency of population transfer resulting from two-step laser excitation followed by resonance fluorescence. In the present investigation, the efficiency of population transfer and fluorescence resulting from the two wavelength excitation scheme used in the cesium resonance fluorescence detection, was experimentally examined by means of absorption and saturation spectroscopy. The purpose of this paper is to analyze

and quantify actual population distributions created in the excited states when the Doppler broadened transition is excited with single-mode laser, and to propose the way to improve low sensitivity of such RFDs, which limits the applicability of these devices. A straightforward way to obtain the quantitative information about the excited state population is to probe the population with another radiation source in the second excitation step. In the present investigation we have employed and tested a simple method for measuring the excited state population that requires only absorption and saturation measurements in a single excitation step.

2. Experimental setup

The experimental setup and two-step excitation scheme used to perform the measurements is shown in Fig. 1. Radiation at 852 nm and 917 nm was provided by external cavity diode lasers operated in Littman–Metcalf configurations (Model TEC 500, Sacher Lasertechnik) with manufacturer specified linewidths of 5 MHz. The excitation was done in Doppler-free geometry i.e. the beams counter-propagated through a room temperature cylindrical cesium absorption cell (Ophos, Inc.) measuring 7.5 cm (or 2.5 cm) in length and 2.5 cm in diameter. The beams had 2 mm in diameter and overlapped along the entire length of the cell. The cell was made of Pyrex glass and was filled with pure cesium metal with no buffer gas added. To scan either laser, a waveform provided by a function generator (Model FG3C, Wavetek Meterman) was used to tune the piezo-driven mirror in the laser cavity. The frequency calibration was achieved by directing a portion of the scanned laser beam into the custom-built confocal FPI with free spectral range (f.s.r.) of 150 MHz. Interference maxima were detected by a photodiode. The radiation transmitted through the cell was directed

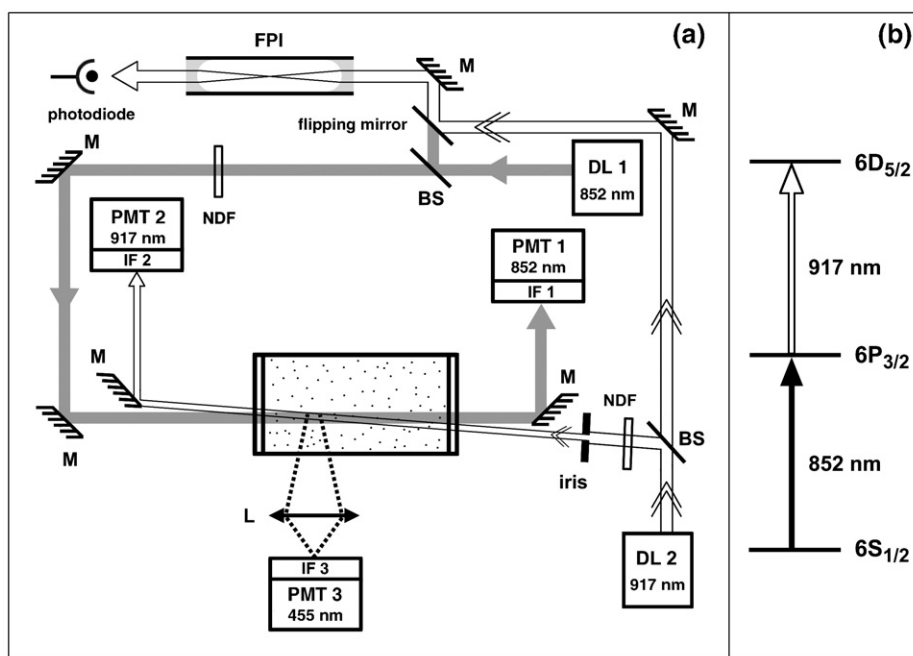


Fig. 1. (a) Setup used to investigate the efficiency of two-step excitation and detection of resonance fluorescence in room temperature cesium vapor. DL=diode laser, PMT=photomultiplier tube, IF=interference filter, M=mirror, BS=beam splitter, L=lens, NDF=neutral density filter. The inclination of the beams in the cell is exaggerated. (b) Two-step excitation scheme used in the present experiment.

into an 852 nm interference filter (Optometrics, LLC) and detected by near-infrared photomultiplier tube (R636, Hamamatsu). Similarly, 917 nm exciting radiation was spatially separated from 852 nm radiation and the excited state absorption was detected by PMT (R5108, Hamamatsu). The PMT output was amplified (Model 427, Keithley Instruments) and recorded by an oscilloscope (TDS3000 Series, Tektronix). Single sequence oscilloscope traces, were stored on a laboratory PC for data analysis.

To determine the saturation behavior of the Doppler broadened $6S_{1/2} \rightarrow 6P_{3/2}$ transition the 852 nm laser was scanned across the transition and absorption spectra at various laser powers in the range of 9 μW to 1.8 mW were recorded. Neutral density filters (Esco Products, Inc.) were used to attenuate the intensity which was measured by a power meter (LaserCheck, Coherent). To determine the population created in the $6P_{3/2}$ state for each 852 nm power used, the 852 nm laser was tuned to the center of the strong hyperfine (h.f.) component of the ground state transition ($6S_{1/2}(F=4) \rightarrow 6P_{3/2}(F=3, 4, 5)$) and the resulting excited state population, as a function of 852 nm power, was probed with 16 μW of 917 nm radiation. Saturation of the homogeneously broadened $6P_{3/2} \rightarrow 6D_{5/2}$ transition was studied by pumping the $6S_{1/2} \rightarrow 6P_{3/2}$ transition in the center of the strong h.f. component with 1.6 mW of 852 nm radiation and measuring 917 nm absorption at powers ranging from 12 μW to 2.5 mW. An excited state absorption experiment capable of probing the $6D_{5/2}$ state population could not be performed as an appropriate laser was not available.

The blue fluorescence at $7P_1 \rightarrow 6S_{1/2}$ transition (455 and 459 nm lines) which emerges in consequence to the radiative $6D_{5/2} \rightarrow 7P_{3/2}$ transfer, was used as a measure of the increase of the population in the $6D_{5/2}$ state during the saturation of the $6P_{3/2} \rightarrow 6D_{5/2}$ transition. The fluorescence at 455 nm was collected at 90° with respect to the laser beams' propagation by means of a lens, and measured by a photomultiplier tube (R928, Hamamatsu) equipped with an interference filter (Optometrics, LLC) centered at 455 nm (FWHM 10 nm). In addition, an observation window (width: 1 cm, height: 2 cm) was used to ensure that always the same region of fluorescence was measured. The photomultiplier output was amplified, recorded by an oscilloscope and stored on a PC for further analysis.

3. Determination of the population densities

The ground state atom number density N was determined from the unsaturated $6S_{1/2}(F=3, 4) \rightarrow 6P_{3/2}(F=2, 3, 4, 5)$ absorption spectrum. From the peak absorption coefficient k_0 of the Doppler profile the ground state density can be obtained using the relation

$$k_0 = \frac{1}{\Delta v_D \sqrt{\pi}} \cdot \frac{\pi e^2}{mc} \cdot N \cdot f \quad (1)$$

where Δv_D is the Doppler constant defined by:

$$\Delta v_D = \frac{v_0}{c} \cdot \sqrt{\frac{2kT}{M}}, \quad (2)$$

f is the oscillator strength of the strong ($F=4 \rightarrow F=3, 4, 5$) or weak ($F=3 \rightarrow F=2, 3, 4$) component of the $6S_{1/2} \rightarrow 6P_{3/2}$ transition ($f_s=0.398$, $f_w=0.310$ [28]), and the remaining symbols have their usual meaning.

Additionally, the ground state density was determined from the integrated unsaturated absorption coefficient according to Ladenburg equation [29]:

$$\int k(v) dv = \frac{\pi e^2}{mc} \cdot N \cdot f \quad (3)$$

The third way to determine N was use of the curve of growth method [29,30]. The value of the experimentally measured equivalent width was in the range corresponding to the linear part of the growth curves where all the curves regardless of the damping parameter value $a = \Delta_L / \Delta_D$ (ratio of the Lorentz to Doppler width) lie practically on the same line. Therefore, it was not necessary to specify a , i.e. to calculate Δ_L from the reduced Cs–Cs broadening parameter $\gamma = \Delta_L / N$ published in [31] and estimated value of N . The mean value of the cesium ground state number density determined in these three ways was found to be $N = (2.4 \pm 0.2) \times 10^{10} \text{ cm}^{-3}$, which is excellent agreement with the density at room temperature (293 K) given by the cesium vapor pressure curve [32,33].

We consider two level system where the state $|2\rangle$ is excited through the $|1\rangle \rightarrow |2\rangle$ transition with monochromatic excitation. The equations to follow will be derived under the following assumptions: the transition is homogeneously broadened, optical pumping (in its classical sense) is absent, and there are no quenching collisions or radiation trapping. The comments on the validity of the obtained relations with respect to optical pumping effects will be made subsequently. If the transition is excited at rate Π which is comparable with the spontaneous relaxation rate A_{21} , the rate equation for the excited steady state population N_2 reads [28]:

$$\frac{dN_2}{dt} = 0 = \Pi N_1 - \frac{g_1}{g_2} \Pi N_2 - A_{21} N_2 \quad (4)$$

In the above relation, g_1 and g_2 are the statistical weights of the lower and upper state, respectively. In the case of a homogeneous line profile, the pumping rate is defined in the following way [28]:

$$\Pi(\delta v_{\text{las}}) = \frac{1}{h\nu_0} \frac{\pi e^2}{mc} f \int P_L(v - v_0) I_v(v - v_0^{\text{las}}) dv \quad (5)$$

where $P_L(v)$ is the normalized Lorentzian line profile, $I_v(v)$ [$\text{J m}^{-2} \text{s}^{-1} \text{Hz}^{-1}$] is the spectral intensity of the laser beam, ν_0^{las} is the central laser frequency, and $\delta v_{\text{las}} = \nu_0 - \nu_0^{\text{las}}$ is the pump detuning from the center of the spectral line. Note that in the above equation $(\pi e^2 f / mc) P(v) = \sigma(v)$ represents the absorption cross section for the considered transition. The pump

rate defined as in Eq. (5) covers all cases of broad as well as narrow band excitation.

Solution to Eq. (4) is obtained in the following form:

$$N_1 = \frac{N}{1 + g_1/g_2} \frac{1 + (g_1/g_2)(1 + S)}{1 + S} \quad (6a)$$

$$N_2 = \frac{N}{1 + g_1/g_2} \frac{S}{1 + S} \quad (6b)$$

where $N = N_1 + N_2$ is the total population of the system and S denotes the saturation parameter given by:

$$S = \frac{\Pi}{A_{21}} \left(1 + \frac{g_1}{g_2} \right) \quad (7)$$

If the transition between states $|1\rangle$ and $|2\rangle$ is inhomogeneously broadened, i.e., if the laser excites atoms with a Maxwell–Boltzmann velocity distribution, not all the atoms are able to absorb the incoming radiation. For the laser propagating in the z -direction, only those atoms with the velocity component v_z being such that the Doppler-shifted laser frequency $\nu' = \nu_{\text{las}} - K_z v_z$ ($K_z = 1/\lambda_{\text{las}}$) falls within the homogeneous linewidth $\Delta\nu_L$ around the central absorption frequency ν_0 of an atom at rest, i.e., $\nu' = \nu_0 \pm \Delta\nu_L$, can significantly contribute to the absorption. If the laser line has a finite width $\Delta\nu_{\text{las}}$, i.e. if $\nu_{\text{las}} = \nu_0^{\text{las}} \pm \Delta\nu_{\text{las}}/2$, the number density $N(v_z)$ of atoms able to absorb the incoming photons is determined by v_z being in the interval between v_z^- and v_z^+ where

$$v_z^\pm = (c/\nu_{\text{las}})(\nu_0^{\text{las}} - \nu_0 \pm (\Delta\nu_L + \Delta\nu_{\text{las}}/2)) \quad (8)$$

With the selected velocity group of atoms taken as conserved during the absorption and emission of a photon, the following relationship is valid:

$$N(v_z) = N_1(v_z) + N_2(v_z) \quad (9)$$

In a Doppler-broadened medium the unsaturated and saturated absorption coefficients, have the following relationship [34]:

$$k^{\text{sat}}(\nu) = \frac{k^{\text{unsat}}(\nu)}{\sqrt{1 + S_0}} \quad (10)$$

where $S_0 = S(\nu_0)$ is the saturation parameter in the center of an inhomogeneously broadened (Gaussian) profile. By expressing S_0 in terms of unsaturated and saturated peak ($k(\nu = \nu_0) = k_0$) absorption coefficients given in Eq. (10), from Eq. (6a) and (b), we obtain the following expressions for the velocity selective population densities in the lower and upper states:

$$N_1(v_z) = \frac{N(v_z)}{1 + g_1/g_2} \left[\frac{g_1}{g_2} + \left(\frac{k_0^{\text{sat}}}{k_0^{\text{unsat}}} \right)^2 \right] \quad (11)$$

$$N_2(v_z) = \frac{N(v_z)}{1 + g_1/g_2} \left[1 - \left(\frac{k_0^{\text{sat}}}{k_0^{\text{unsat}}} \right)^2 \right] \quad (12)$$

As implied in the starting assumptions, the above equations will yield valid results only in the case when the increased transparency of the medium is solely due to the transition saturation. Namely, when the system with multiple ground states that are accessible from the excited states is illuminated with polarized light of adequate intensity there are two distinct processes that may contribute to the depletion of the particular ground state hyperfine level: saturation and hyperfine pumping [35]. In the presence of hyperfine pumping the two level model considered above would represent an open system with the possibility for atoms to accumulate in the other ground state component and the assumption $N = N_1 + N_2$ would not hold any more. Also the inclusion of the relaxation rate to the other ground state level would be necessary in the denominator of the saturation parameter (Eq. (7)).

Considering the structure of the strong h.f. component $6S_{1/2}(F=4) \rightarrow 6P_{3/2}(F=3, 4, 5)$ of the Cs D2 line at room temperature [28] one can see that the pumping in its center dominantly excites closed $6S_{1/2}(F=4) \rightarrow 6P_{3/2}(F=5)$ h.f. transition. There is also a small probability of exciting atoms on the next neighbour, open or cycling $6S_{1/2}(F=4) \rightarrow 6P_{3/2}(F=4)$ transition which is around 250 MHz apart. Atoms undergoing this transition can subsequently decay to the other ground state $6S_{1/2}(F=3)$. No optical pumping can take place on the closed transition, while weak excitation of the cycling transition can to some extent result with optical pumping. As shown in [35] for the case of rubidium, the transmission of the medium in the center of the Doppler envelope of the strong h.f. component of the Rb D2 line due to hyperfine pumping alone amounts to $\approx 5\%$. In the case of cesium we can expect this effect to be even less pronounced because the closest cycling transition is separated from the closed one by twice as much as in the rubidium case.

As for the weak $6S_{1/2}(F=3) \rightarrow 6P_{3/2}(F=2, 3, 4)$ component of the Cs D2 line, the pumping in the center of the Doppler envelope coincides with excitation of the open $6S_{1/2}(F=3) \rightarrow 6P_{3/2}(F=3)$ transition and it can be expected that the measured value k_0^{sat} of the peak absorption coefficient will be affected by the optical pumping effect.

Therefore, in the present experiment, Eqs. (11) and (12) were applied only to the Doppler broadened absorption spectrum of the strong h.f. component of the $6S_{1/2} \rightarrow 6P_{3/2}$ transition. In the calculation the value $(g_1/g_2)_S = 8/9$ (see Appendix) was used for the ratio of the statistical weights of the involved levels.

The fraction $N(v_z)$ of the atoms in the lower state that are able to absorb under inhomogeneous broadening conditions can be determined according to [28]:

$$N(v_z, \delta\nu_{\text{las}}, \Delta\nu_{\text{las}}) = 4\sqrt{\frac{\ln 2}{\pi}} e^{-4\ln 2(\delta\nu_{\text{las}}/\Delta\nu_G)^2} \frac{\Delta\nu_{\text{H}}^{\text{sqr}} + \Delta\nu_{\text{las}}/2}{\Delta\nu_G} N \quad (13)$$

Here $\delta\nu_{\text{las}} = 0$ since the pumping was done in the line center, $\Delta\nu_G$ is the inhomogeneous (Doppler) width (FWHM) of the profile, $\Delta\nu_{\text{H}}^{\text{sqr}}$ is a width of the rectangular approximation to the normalized homogenous (Lorentz) component of the line profile, and N is the total lower state population. Eq. (13) is valid when the line profile is nearly pure Doppler

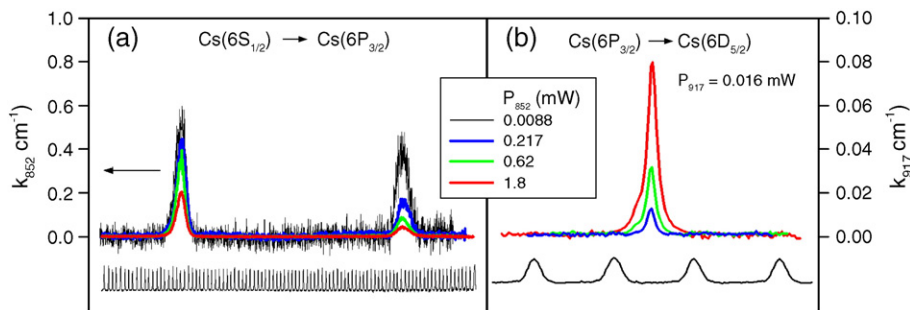


Fig. 2. (a) Absorption coefficient of the $6S_{1/2} \rightarrow 6P_{3/2}$ transition measured for several powers P_{852} of 852 nm radiation. (b) Absorption coefficient of the $6P_{3/2}(F=2, 3, 4, 5) \rightarrow 6D_{5/2}(F=1, 2, 3, 4, 5, 6)$ transition measured with 852 nm laser being locked at the center of the strong hyperfine component $6S_{1/2}(F=4) \rightarrow 6P_{3/2}(F=3, 4, 5)$ of the first excitation step. Measurements were done for a series of P_{852} values and the population created in the excited $6P_{3/2}$ state was probed with attenuated 917 nm laser having the power of $P_{917} = 16 \mu\text{W}$. The frequency dispersion was calibrated by the transmission peaks of the confocal Fabry–Perot interferometer with f.s.r. of 150 MHz.

($\Delta v_{\text{H}}^{\text{SQR}} \ll \Delta v_{\text{G}}$) and the laser linewidth Δv_{las} is much smaller than the inhomogeneous linewidth but comparable with the homogeneous linewidth. These criteria were fulfilled in the present experiment, since $\Delta v_{\text{G}} = 460$ MHz (measured width of the Doppler envelope of the strong h.f. component), $\Delta v_{\text{las}} = 5$ MHz and $\Delta v_{\text{H}}^{\text{SQR}} = 8$ MHz. The value of $\Delta v_{\text{H}}^{\text{SQR}}$ was obtained from the relation $\Delta v_{\text{H}}^{\text{SQR}} = 1/P_{\text{L}}(v_0)$, where $P_{\text{L}}(v_0) = 2/(\pi \Delta v_{\text{L}})$ is the peak value of the normalized Lorentz profile. In the experiment at hand, the Lorentz width was $\Delta v_{\text{L}} = \Delta v_{\text{N}} + \gamma_{\text{Cs-Cs}} N = 5.2$ MHz ($\Delta v_{\text{N}} = 5.18$ MHz [36]). The value of $N(v_2)$ determined from Eq. (13) amounts to $1 \times 10^9 \text{ cm}^{-3}$.

Population in the $6P_{3/2}$ level obtained from the saturation measurements using Eq. (12), was also determined by the absorption measurement in the second excitation step $6P_{3/2} \rightarrow 6D_{5/2}$ ($\lambda = 917$ nm). In these measurements the power of the 917 nm laser was sufficiently low to probe the population of interest without introducing any additional perturbation. The $6S_{1/2} \rightarrow 6P_{3/2}$ transition was pumped in the center of the strong h.f. component and the second step laser was swept in frequency across $6P_{3/2} \rightarrow 6D_{5/2}$ transition. The 917 nm scans were taken for a series of 852 nm laser powers already applied in the saturation experiment. The $6P_{3/2}$ number density was determined from the integrated or peak value of the unsaturated absorption coefficient k_{917} . Since the scanned frequency range covered $6P_{3/2}(F=3, 4, 5) \rightarrow 6D_{5/2}(F=2, 3, 4, 5, 6)$ transitions, the evaluation of $N(6P_{3/2})$ from the integrated $k_{917}(v)$ was done using Eq. (3) and the corresponding oscillator strength $f_{917} = 0.238$ obtained (see Appendix) from the total oscillator strength $f_{917}^{\text{tot}} = 0.282$ [37] of the $6P_{3/2} \rightarrow 6D_{5/2}$ transition. The $k_{917}(v)$ spectra were obtained with two-step excitation in counter-propagating configuration and the measured line profiles were Doppler-free, i.e. exhibited the pure Lorentzian shape. Thus for the evaluation of $N(6P_{3/2})$ from the measured peak absorption coefficient the expression for the peak value of the Lorentzian profile was used:

$$k_0^{\text{L}} = \frac{\pi e^2}{mc} \cdot N \cdot f_{917} \cdot \frac{2}{\pi \Gamma} \quad (14)$$

where the line width Γ (FWHM) was determined from the measured spectra. Very good agreement between $N(6P_{3/2})$ values obtained in these two ways was found.

For a homogeneously broadened $|1\rangle \rightarrow |2\rangle$ transition, the relationship between the unsaturated (k^{unsat}) and saturated (k^{sat}) peak absorption coefficients, measured at very low and relatively high laser power, respectively, is given by [28,34]:

$$k^{\text{sat}}(v) = \frac{k^{\text{unsat}}(v)}{1 + S(v)} \quad (15)$$

The above equation yields the following expression for the ratio of the unsaturated and saturated peak ($v = v_0$) absorption coefficients of the homogeneously broadened transition:

$$\frac{k_0^{\text{sat}}}{k_0^{\text{unsat}}} = \frac{1}{1 + S_0} \quad (16)$$

By using Eqs. (16), (6a) and (b) one obtains the following expressions for the populations of the lower and upper state:

$$N_1 = \frac{N}{1 + g_1/g_2} \left(\frac{g_1}{g_2} + \frac{k_0^{\text{sat}}}{k_0^{\text{unsat}}} \right) \quad (17)$$

$$N_2 = \frac{N}{1 + g_1/g_2} \left(1 - \frac{k_0^{\text{sat}}}{k_0^{\text{unsat}}} \right) \quad (18)$$

From the measurements of the peak absorption coefficient for a series of laser powers the population densities N_1 and N_2 of the initial and final state, respectively, as functions of the applied power can be determined using the above equations. In the present experiment Eqs. (17) and (18) are applicable to the determination of the population transfer from $6P_{3/2}$ to $6D_{5/2}$ state.

4. Results and discussion

The quantum efficiency of RFD/RFID devices depends on the efficiency of the population conversion between input (excitation) and output (detection) channel. For the cesium based RFD/RFID [13,27] operating at room temperature in pure vapor, which uses $6D_{5/2} \rightarrow 7P_{3/2} \rightarrow 6S_{1/2}$ radiative decay scheme to detect the initial absorption event occurring at $6S_{1/2} \rightarrow 6P_{3/2}$ transition, the detection efficiency essentially depends on the

population density of the $6D_{5/2}$ state which can be created with two-step $6S_{1/2} \rightarrow 6P_{3/2} \rightarrow 6D_{5/2}$ excitation.

The efficiency of the first step excitation was examined by measurements of the laser absorption at $6S_{1/2}(F=4) \rightarrow 6P_{3/2}(F=3, 4, 5)$ transition. The transition was gradually saturated and the measured peak absorption coefficients of the strong h.f. component was used to determine the population densities in the $6S_{1/2}$ and $6P_{3/2}$ states using Eqs. (11) and (12). The values thus obtained for the $6P_{3/2}$ density were checked by measuring the unsaturated $6P_{3/2} \rightarrow 6D_{5/2}$ absorption and determining $N(6P_{3/2})$ from Eqs. (3) or (14).

The results of the measurements of the absorption coefficient k_{852} at the $6S_{1/2}(F=3, 4) \rightarrow 6P_{3/2}(F=2, 3, 4, 5)$ transition are shown in Fig. 2a for several pump powers P_{852} in the investigated range ($9 \mu\text{W} \leq P_{852} \leq 1.8 \text{ mW}$). For the two lowest applied powers (9 and 50 μW) the spectrum was measured in a 2.5 cm long cell to avoid total absorption in the line center, while the remaining scans were taken in the cell having $L=7.5 \text{ cm}$. The frequency calibration marks in Fig. 2a and b were separated by 150 MHz.

The measurements were done at a cesium ground state number density of $N=(2.4 \pm 0.2) \times 10^{10} \text{ cm}^{-3}$ which was determined from the unsaturated absorption spectrum ($P_{852}=9 \mu\text{W}$) as described previously. The velocity selected populations $N_1(v_z)$ and $N_2(v_z)$ of the $6S_{1/2}$ and $6P_{3/2}$ states, respectively, created with different laser pump power applied, were obtained from the measured peak absorption coefficient of the strong ($F=4 \rightarrow F'=3, 4, 5$) h.f. of the $6S_{1/2} \rightarrow 6P_{3/2}$ transition using Eqs. (11), (12) and (13).

The dependence of the $N_2(v_z)$ population on the power P_{852} of the pump laser, determined from the saturation measurements in the first excitation step were checked by directly probing the $6P_{3/2}$ state density with weak ($P_{917}=16 \mu\text{W}$) second step laser at $6P_{3/2} \rightarrow 6D_{5/2}$ transition. The 852 nm laser was locked in the center of the strong h.f. component of the D2 line, and its power was varied in the range from 9 μW to 1.8 mW. For each P_{852} power the 917 nm laser was scanned over $6P_{3/2}(F=4, 5) \rightarrow 6D_{5/2}(F=3, 4, 5, 6)$ transition and the unsaturated upper step absorption was recorded. For the two lowest applied P_{852} powers the upper state absorption was too weak to be measured (the cell had to be kept short to avoid optical thickness of the 852 nm line). Reliable signals were obtained for $P_{852} > 200 \mu\text{W}$, and the results for the absorption coefficient k_{917} are shown in Fig. 2b for a few values of the pump power P_{852} .

Because the $k_{917}(v)$ measurements were performed with two-step excitation in counter-propagating beam configuration the obtained $k_{917}(v)$ profile is Doppler-free and has the Lorentzian form. The displayed $k_{917}(v)$ spectra exhibit unresolved components of the $6P_{3/2}(F=4, 5) \rightarrow 6D_{5/2}(F=3, 4, 5, 6)$ transition. The most pronounced peaks separated by $\approx 30 \text{ MHz}$, correspond to $F=5 \rightarrow F'=5, 6$ h.f. transitions [38,39]. The measured $k_{917}(v)$ confirms the expectation expressed previously in Section 2, i.e. that in the present experimental conditions only the $6P_{3/2}(F=5)$ level is populated significantly when the strong h.f. component is excited in its center with a narrow band laser. The number density $N_2(v_z)$ of the atoms in the $6P_{3/2}$ state was calculated from the measured

$k_{917}(v)$ in two ways: from the peak absorption coefficient of the Lorentzian profile (Eq. (14)) and from the integrated absorption coefficient (Eq. (3)), which yielded consistent results. The corresponding number density $N_1(v_z)$ of the velocity selected fraction of the atoms in the ground state was calculated as $N_1(v_z) = N(v_z) - N_2(v_z)$, where $N(v_z)$ is given by Eq. (13).

The values of $N_1(v_z)$ and $N_2(v_z)$ obtained by direct probing of the excited state population with second step laser as a function of pump power P_{852} are depicted in Fig. 3 with full symbols, while the results determined from the saturation of the strong h.f. component in the first excitation step are depicted with open symbols. The agreement between the results obtained in these two ways is very good. As mentioned in Section 2 the absorption coefficient of $6S_{1/2} \rightarrow 6P_{3/2}$ transition might be burdened with optical pumping effects. However, as anticipated earlier, and confirmed with the obtained agreement, it turns out that within the error bar of the measured data, pumping in the center of the strong h.f. component of the Cs $6S_{1/2} \rightarrow 6P_{3/2}$ transition may be considered to be free of such effects. Based on this finding we may conclude that reliable determination of the excited state population is possible by performing saturation spectroscopy in a single excitation step, with a care being taken that the excitation is done on the closed transition. This is very convenient in the cases when lacking adequate laser to further excite atoms in the upper state.

The population created in the $6D_{5/2}$ state with the 917 nm laser was determined from saturation measurements at the $6P_{3/2} \rightarrow 6D_{5/2}$ transition. With the 852 nm laser (power: 1.56 mW) being locked to the center of the strong h.f. component of the D2 line, the upper step absorption was measured for a series of P_{917} powers between 12 μW and 2.5 mW. The $k_{917}(v)$ results for four P_{917} values covering the investigated range are shown in Fig. 4. Description of

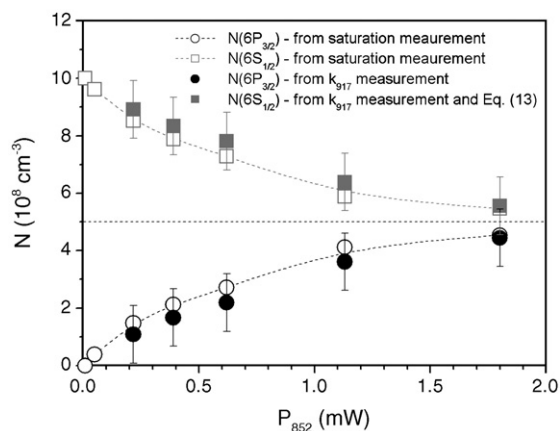


Fig. 3. The velocity selective portions of the ground $N(6S_{1/2})$ and the excited $N(6P_{3/2})$ state populations created during the saturation of the Cs $6S_{1/2}(F=4) \rightarrow 6P_{3/2}(F=3, 4, 5)$ transition at 852 nm, plotted against applied pump power P_{852} . ● — Atom number density of the $6P_{3/2}$ state determined from $6P_{3/2} \rightarrow 6D_{5/2}$ absorption measurements; ○ — atom number density of the $6P_{3/2}$ state determined from the saturation of the $6S_{1/2}(F=4) \rightarrow 6P_{3/2}(F=3, 4, 5)$ transition; □ — velocity selected fraction of the ground state population $N(6S_{1/2})$ determined from the saturation measurement; ■ — velocity selected fraction of the ground state population $N(6S_{1/2})$ determined using the measured data for $N(6P_{3/2})$ and the calculated value for the total number of the atoms in the lower state that are able to absorb 852 nm radiation (Eq. (13)). Dashed lines are only guides to the eye.

the measured spectra is given in Fig. 2b. The peak absorption coefficients of the unsaturated and saturated spectra were used to evaluate $N(6P_{3/2})$ and $N(6D_{5/2})$ according to Eqs. (17) and (18), respectively. The value of initial population created in the $6P_{3/2}$ state was additionally evaluated by determining $N(6P_{3/2})$ from the unsaturated $k_{917}(v_0)$ measurement according to Eq. (14). The $N(6P_{3/2})$ and $N(6D_{5/2})$ populations dependence on the applied P_{917} power are shown in Fig. 5.

During saturation of the $6P_{3/2} \rightarrow 6D_{5/2}$ transition, for each applied P_{917} power the blue fluorescence at $7P_J \rightarrow 6S_{1/2}$ (455 and 459 nm lines) was recorded simultaneously with the upper step absorption. It served as indication of the increased population in the $6D_{5/2}$ state. The $7P_J$ state can be populated radiatively from $6P_J$ level and by collisional $7P$ – $6D$ mixing induced by Cs ground state atoms. To our knowledge the cross sections for this process have not been reported. If we assume that they are two orders of magnitude larger than the cross sections for the same process induced by noble gases (He, Ar) [40], which is very likely overestimated, the corresponding $7P$ – $6D$ collisional transfer rate at the present cesium density ($2.4 \times 10^{10} \text{ cm}^{-3}$) would be $\approx 20 \text{ s}^{-1}$ at most. Compared with the radiative $6D_J \rightarrow 7P_J$ rates which are of the order of magnitude of 10^4 s^{-1} [28] these collisional rates are negligible. Therefore, we may say that in the present experimental conditions the creation of the $7P_J$ population is entirely due to weak radiative $6D_J \rightarrow 7P_J$ relaxation. Considering the cross sections [41] for the cesium-induced collisional mixing of the $6D_J$ fine structure levels, the losses in the $6D_{5/2}$ population due to this process can also be neglected in comparison with the radiative $6D_{5/2} \rightarrow 7P_{3/2}$ rate. Collisional $7P_J$ fine-structure mixing is also very weak at the present ground state Cs density (see the corresponding cross sections in [42]), and with the used interference filter (FWHM 10 nm), the measured fluorescence intensity can be entirely attributed to the 455 nm line. Taking into account all the information mentioned above, it is justified to use the intensity of the measured blue fluorescence as a measure of the $6D_{5/2}$ population.

In Fig. 6 the dependence of the 455 nm line fluorescence intensity is plotted against the population in the $6D_{5/2}$ level determined from the saturation of the upper excitation step. As

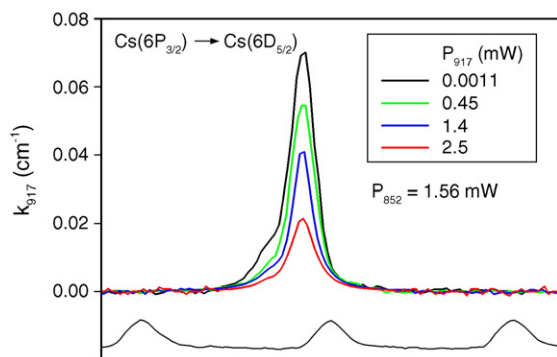


Fig. 4. Absorption coefficient of the $6P_{3/2} \rightarrow 6D_{5/2}$ transition measured for several powers P_{917} of 917 nm radiation. The measurements were taken with the pump laser being locked at the center of the strong hyperfine component $6S_{1/2}$ ($F=4$) \rightarrow $6P_{3/2}$ ($F=3, 4, 5$). The pump laser power was $P_{852} = 1.56 \text{ mW}$. The spectrum calibration marks are separated by 150 MHz.

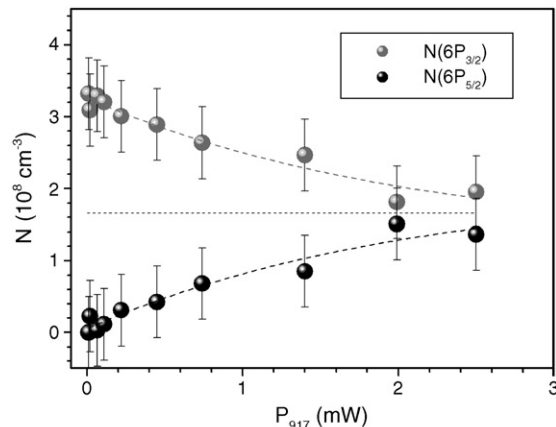


Fig. 5. The $6P_{3/2}$ and the $6D_{5/2}$ state populations created during the saturation of the Cs $6P_{3/2} \rightarrow 6D_{5/2}$ transition at 917 nm, plotted against applied pump power P_{917} . The data were obtained from the measurements of the peak absorption coefficient k_{917} while saturating $6P_{3/2} \rightarrow 6D_{5/2}$ transition. ● — Atom number density of the $6D_{5/2}$ state; ● — atom number density of the $6P_{3/2}$ state. Dashed lines are only to guide the eye.

can be seen the measured five-fold increase in the fluorescent intensity corresponds to a change of $N(6D_{5/2})$ by the same factor. This can serve as confirmation of the reliability of the method used for the determination of the excited state populations created with two-step excitation, using single-mode narrow band lasers.

The performed measurements illustrate and quantify the limitations on the size of the excited state population which can be created with pumping the Doppler broadened line with a single-mode narrow-line laser. With the ground state atom number density amounting to $2.4 \times 10^{10} \text{ cm}^{-3}$ and with complete saturation of the velocity selected group of atoms $N(v_z)$, a maximum density of $\approx 5 \times 10^8 \text{ cm}^{-3}$ in the $6P_{3/2}$ state can be attained, i.e. only $\approx 2\%$ of the ground state population can be transferred to the first excited state. Our finding is in agreement with general expectations that the excited state populations created by narrow-band laser pumping in the Doppler profile are small. A rough estimate of the fraction of atoms that can be

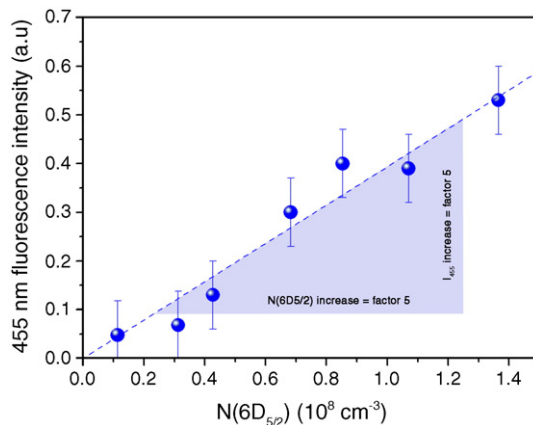


Fig. 6. The intensity of the blue fluorescence emerging at the $7P_{1/2, 3/2} \rightarrow 6S_{1/2}$ transition subsequent to the radiative $6D_{5/2} \rightarrow 7P_{3/2}$ transfer of population, plotted in dependence on the atom number density created in $6D_{5/2}$ state by $6P_{3/2} \rightarrow 6D_{5/2}$ pumping. The shaded triangle indicates that the increase in the $N(6D_{5/2})$ population increases the 455 nm fluorescent signal by the same factor.

excited by the saturation of the transition can be obtained from the ratio of the homogeneous and the inhomogeneous widths. In the present case, such an estimation yields an excited state population which amounts to $\approx 1\%$ of the ground state population. This assessment underestimates the actual excited state population because it does not take into account the ratio of the laser width to the homogeneous width, which does not necessarily has to be small. In the experiment at hand, the velocity selective population fraction was calculated using Eq. (13) which takes into account the homogeneous and inhomogeneous broadening as well as the laser line width and pump detuning. The very good agreement obtained with the experimental values proves the validity of our approach.

With the second excitation step and its complete saturation, eventually only $\approx 1\%$ of the ground state population can be transferred to the $6D_{5/2}$ state. Moreover, these few atoms reaching the $6D_{5/2}$ state have to pass another obstacle before exiting the $7P_{3/2} \rightarrow 6S_{1/2}$ (detection) channel. Namely, the radiative $6D_{5/2} \rightarrow 7P_{3/2}$ transition acts as a “bottle neck” in the considered excitation scheme, due to its small transition probability. All these inconveniences manifest themselves in a low quantum efficiency of resonance fluorescence imaging detectors which employ single-mode lasers to maintain high spectral resolution, and low vapor pressure conditions (Doppler-broadened lines) to avoid radiation diffusion and trapping which deteriorate spatial resolution. In fact, the quantum efficiency of the process is determined by the branching ratio between the radiative transition rate to the fluorescing level ($7P_{3/2}$) and the sum of the de-excitation rates of the $D_{5/2}$ level. By using the A -values reported in the literature for the pertinent transitions (see [27]), this efficiency is ~ 0.004 , and therefore even lower than the population transfer efficiency into the $6D_{5/2}$ state. Therefore, in order to preserve the advantages of high spectral and spatial resolution for the investigated Cs RFID, and at the same time increase its quantum efficiency, it becomes imperative to ensure efficient $6D \rightarrow 7P$ population transfer. A way of achieving this has already been proposed and investigated [27]. By introducing helium in the system, a 35-fold quantum efficiency increase was obtained. The helium induced substantial collisional $6D \rightarrow 7P$ mixing and thus augmented the population transfer on one hand, and on the other caused line broadening and therefore increased the effective pumping rate in the first excitation step.

5. Conclusion

The limitations of velocity selective excitation by pumping the Doppler broadened atomic line with a single-mode narrow-line laser have been examined quantitatively. The use of excited state absorption in combination with saturation theory has allowed the development of a robust technique for monitoring the transfer of atomic populations within a multi-level atomic system. It has been shown that velocity-selective excitation, in addition to saturation effects, can greatly influence the transfer of population involved in a two-step excitation scheme followed by detection of resonance fluorescence, which is used in a cesium based resonance fluorescence detector.

Acknowledgements

This research was supported by NIH Grant 63965-04 and the Ministry of Science, Education and Sport of the Republic of Croatia. V. Horvatic would like to thank the Department of Chemistry, University of Florida in Gainesville for providing her with the opportunity of a working stage and for the kind hospitality.

Appendix A

The oscillator strength for the cesium $6S_{1/2} \rightarrow 6P_{3/2}$ transition is $f=0.708$ [36]. If the hyperfine structure of the $6S_{1/2}$ and $6P_{3/2}$ levels is taken into account, there are six transitions involved, and the following relationship between the corresponding oscillator strengths exists:

$$f_a + f_b + f_c = f_d + f_e + f_f = f = 0.708 \quad (\text{A.1})$$

Here f_a , f_b , and f_c label the oscillator strengths for $F=3 \rightarrow F=2$, 3, 4 transitions, respectively, which form the weak component of the $6S_{1/2} \rightarrow 6P_{3/2}$ line. The oscillator strengths for $F=4 \rightarrow F=3$, 4, 5 transitions, which constitute the strong component of the transition are denoted with f_d , f_e , and f_f , respectively.

If we look at the ground state as a whole, the oscillator strengths of the weak and the strong component of $6S_{1/2} \rightarrow 6P_{3/2}$ transition are defined by:

$$f_w = g_{F=3}(f_a + f_b + f_c) = g_{F=3} f = 0.310$$

$$f_s = g_{F=4}(f_d + f_e + f_f) = g_{F=4} f = 0.398 \quad (\text{A.2})$$

where $g_{F=3}=7/16$ and $g_{F=4}=9/16$ are the relative statistical weights of the ground state hyperfine sublevels with $F=3$ and $F=4$, respectively.

The oscillator strength of the $|1\rangle \rightarrow |2\rangle$ transition is given by [29]:

$$f_{12} = \frac{mc}{8\pi^2 e^2} \lambda_{12}^2 \frac{g_2}{g_1} A_{21} \quad (\text{A.3})$$

Accordingly, we can define the oscillator strengths for the weak and strong component of the $6S_{1/2} \rightarrow 6P_{3/2}$ transition:

$$f_w = \frac{mc}{8\pi^2 e^2} \lambda_{12}^2 \left(\frac{g_2}{g_1}\right)_w A_{21} \quad f_s = \frac{mc}{8\pi^2 e^2} \lambda_{12}^2 \left(\frac{g_2}{g_1}\right)_s A_{21} \quad (\text{A.4})$$

By taking the ratios f_w/f_{12} and f_s/f_{12} , and taking into account Eq. (A.2) we obtain:

$$\left(\frac{g_2}{g_1}\right)_w = g_{F=3} \frac{g_2}{g_1} \quad \left(\frac{g_2}{g_1}\right)_s = g_{F=4} \frac{g_2}{g_1} \quad (\text{A.5})$$

For the $6S_{1/2} \rightarrow 6P_{3/2}$ transition, $g_1=2$ and $g_2=4$, and the relation (A.5) yields $(g_2/g_1)_w=7/8$ and $(g_2/g_1)_s=9/8$ for the ratio of the statistical weights of the upper and lower level in the case

of weak and strong hyperfine component of the $6S_{1/2} \rightarrow 6P_{3/2}$ line, respectively.

By applying the expressions for the relative line intensities of the $(J, F) \rightarrow (J', F')$ hyperfine transitions [28] to the Cs $6P_{3/2}(F=2, 3, 4, 5) \rightarrow 6D_{5/2}(F=1, 2, 3, 4, 5, 6)$ case (917 nm line), the following relationship between the intensities $I_{FF'} = I(F \rightarrow F')$ of the considered hyperfine components is found:

$$\begin{aligned} I_{21} : I_{22} : I_{23} : I_{32} : I_{33} : I_{34} : I_{43} : I_{44} : I_{45} : I_{54} : I_{55} : I_{56} \\ = \frac{3}{13} : \frac{3}{13} : \frac{3}{26} : \frac{2}{13} : \frac{35}{104} : \frac{33}{104} : \frac{9}{104} : \frac{891}{2600} \\ : \frac{198}{325} : \frac{21}{650} : \frac{77}{13} : 1 \end{aligned} \quad (\text{A.6})$$

If the total oscillator strength for the $J \rightarrow J'$ transition is known, the oscillator strength of each particular hyperfine transition can be obtained from the set of the following relations [28]:

$$\frac{I(F \rightarrow F')}{I(\hat{F} \rightarrow \hat{F}')} = \frac{f(F \rightarrow F')}{f(\hat{F} \rightarrow \hat{F}')} \cdot \frac{2F + 1}{2\hat{F} + 1} \quad (\text{A.7})$$

$F, \hat{F}, \hat{F}' = F', F' \pm 1$

For the Cs $6P_{3/2}(F=3, 4, 5) \rightarrow 6D_{5/2}(F=2, 3, 4, 5, 6)$ hyperfine transitions, which were relevant for the evaluation of present experimental results, the corresponding oscillator strengths calculated using Eq. (A.7) read:

$$\begin{aligned} f_{32} = 0.054 \quad f_{43} = 0.024 \quad f_{54} = 0.007 \\ f_{33} = 0.117 \quad f_{44} = 0.093 \quad f_{55} = 0.053 \\ f_{32} = 0.111 \quad f_{45} = 0.165 \quad f_{56} = 0.222 \end{aligned} \quad (\text{A.8})$$

If each hyperfine sublevel of the $6P_{3/2}$ state is considered, the following relationship between the oscillator strengths of the hyperfine transitions holds:

$$\begin{aligned} f_{21} + f_{22} + f_{23} = f_{32} + f_{33} + f_{34} = f_{43} + f_{44} + f_{45} \\ = f_{54} + f_{55} + f_{56} = f_{917}^{\text{tot}} \end{aligned} \quad (\text{A.9})$$

where the total oscillator strength for the 917 nm line is $f_{917}^{\text{tot}} = 0.282$ [37].

If we look at the $6P_{3/2}$ state as a whole, the oscillator strengths of $F \rightarrow F, F \pm 1$ components are:

$$\begin{aligned} f_3 = g_{F=3}(f_{32} + f_{33} + f_{34}) \\ f_4 = g_{F=4}(f_{43} + f_{44} + f_{45}) \\ f_5 = g_{F=5}(f_{54} + f_{55} + f_{56}) \end{aligned} \quad (\text{A.10})$$

where $g_F = (2F + 1)/g_{\text{tot}}$ denotes the relative statistical weight of the considered hyperfine sublevel of the $6P_{3/2}$ state, and $g_{\text{tot}} = 32$ is the total statistical weight of the $6P_{3/2}$ state.

The relation (A.10) yields the oscillator strength $f_{917} = f_3 + f_4 + f_5 = 0.238$ for the $6P_{3/2}(F=3, 4, 5) \rightarrow 6D_{5/2}(F=2, 3, 4, 5, 6)$ component of the $6P_{3/2} \rightarrow 6D_{5/2}$ transition.

References

- [1] P.G. Pappas, M.M. Bums, D.D. Hinshelwood, M.S. Feld, Saturation spectroscopy with laser optical pumping in atomic barium, *Phys. Rev.*, A 21 (1955) (1980) 1955–1968.
- [2] C.S. Adams, A.I. Ferguson, Saturated spectroscopy and two-photon absorption spectroscopy in rubidium using an actively stabilised Ti:Al₂O₃ ring laser, *Opt. Commun.* 75 (1990) 419–424.
- [3] E. Kuchta, R.J. Alvarez, Y.H. Li, D.A. Krueger, C.Y. She, Collisional broadening of Ba I line (553.5 nm) by He or Ar, *Appl. Phys.*, B 50 (1990) 129–132.
- [4] K.-D. Heber, P.J. West, E. Mathias, Pressure shift and broadening of Sr i Rydberg states in noble gases, *Phys. Rev.*, A 37 (1988) 1438–1448.
- [5] V.S. Letokhov, M.A. Ol'shanii, Yu. B. Ovchinnikov, Laser cooling of atoms: a review, *Quantum Semiclassical Opt.* 7 (1995) 5–40.
- [6] A. Marks, A.P. Hickman, A.D. Streater, J. Huennekens, Thermalization of fast cesium $5D_{3/2}$ atoms in collisions with ground-state cesium atoms, *Phys. Rev.*, A 71 (2005) 012711 (1)–012711 (14).
- [7] O.I. Matveev, B.W. Smith, J.D. Winefordner, A low pressure mercury vapor resonance ionization image detector, *Appl. Phys. Lett.* 72 (1998) 1673–1675.
- [8] A.A. Podshivalov, W.L. Clevenger, O.I. Matveev, B.W. Smith, J.D. Winefordner, Distortion-free microchannel plate mercury atomic resonance ionization image detector, *Appl. Spectrosc.* 54 (2000) 175–180.
- [9] D. Pappas, O.I. Matveev, B.W. Smith, M.R. Shepard, A.A. Podshivalov, J.D. Winefordner, Sealed-cell mercury resonance ionization imaging detector, *Appl. Opt.* 39 (2000) 4911–4917.
- [10] A.A. Podshivalov, M.R. Shepard, O.I. Matveev, B.W. Smith, J.D. Winefordner, Ultrahigh-resolution, frequency-resolved resonance fluorescence imaging with a monoisotropic mercury atom cell, *J. Appl. Phys.* 86 (1999) 5337–5341.
- [11] J.P. Temirov, N.P. Chigarev, O.I. Matveev, N.O. Omenetto, B.W. Smith, J.D. Winefordner, A resonance ionization imaging detector based on cesium atomic vapor, *Spectrochim. Acta Part B* 59 (2004) 677–687.
- [12] E. Korevaar, M. Rivers, C.S. Liu, Imaging atomic line filter for satellite tracking, *SPIE Space Sensing, Communications, and Networking*, vol. 1059, 1989, pp. 111–118.
- [13] D. Pappas, N.C. Pixley, O.I. Matveev, B.W. Smith, J.D. Winefordner, A cesium resonance fluorescence imaging monochromator, *Opt. Commun.* 191 (2001) 263–269.
- [14] D. Pappas, N.C. Pixley, B.W. Smith, J.D. Winefordner, Diffusion of resonance radiation in atomic vapor imaging, *Spectrochim. Acta Part B* 56 (2001) 1761–1767.
- [15] D. Pappas, T.L. Correll, N.C. Pixley, B.W. Smith, J.D. Winefordner, Detection of Mie scattering using a resonance fluorescence monochromator, *Appl. Spectrosc.* 56 (2002) 1237–1240.
- [16] N.C. Pixley, T.L. Correll, D. Pappas, O.I. Matveev, B.W. Smith, J.D. Winefordner, Tunable resonance fluorescence monochromator with sub-Doppler spectral resolution, *Opt. Lett.* 26 (2001) 1946–1948.
- [17] N.C. Pixley, T.L. Correll, D. Pappas, B.W. Smith, J.D. Winefordner, Sub-Doppler spectral resolution and improved sensitivity in a cesium resonance fluorescence imaging monochromator, *Appl. Spectrosc.* 56 (2002) 677–681.
- [18] N.C. Pixley, T.L. Correll, D. Pappas, N. Omenetto, B.W. Smith, J.D. Winefordner, Moving object detection using a cesium resonance fluorescence monochromator, *Opt. Commun.* 219 (2003) 27–31.
- [19] S. Knezovic, C. Vadla, M. Movre, Fine structure excitation transfer between the potassium 4^2P states induced by collisions with caesium atoms, *Z. Phys., D At. Mol. Clust.* 22 (1992) 449–450.
- [20] C. Vadla, S. Knezovic, M. Movre, Rubidium 5^2P fine-structure transitions induced by collisions with potassium and caesium atoms, *J. Phys.*, B 25 (1992) 1337–1345.
- [21] C. Vadla, M. Movre, V. Horvatic, Sodium $3P$ fine-structure excitation transfer induced by collisions with rubidium and caesium atoms, *J. Phys.*, B 27 (1994) 4611–4622.

- [22] C. Vadla, K. Niemax, V. Horvatic, R. Beuc, Population and deactivation of lowest lying barium levels by collisions with He, Ar, Xe and Ba ground state atoms, *Z. Phys., D At. Mol. Clust.* 34 (1995) 171–184.
- [23] C. Vadla, V. Horvatic, The $6s5d\ ^1D_2 \rightarrow 6s5d\ ^3D_J$ excitation energy transfer in barium induced by collisions with He, Ar and Xe atoms, *Fizika A* 4 (1995) 463–472.
- [24] V. Horvatic, C. Vadla, M. Movre, The collision cross sections for excitation energy transfer in $Rb^*(5P_{3/2})+K(4S_{1/2}) \rightarrow Rb(5S_{1/2})+K^*(4P_J)$ processes, *Z. Phys., D At. Mol. Clust.* 27 (1993) 123–130.
- [25] V. Horvatic, D. Veza, M. Movre, K. Niemax, C. Vadla, Collision cross sections for excitation energy transfer in $Na^*(3P_{1/2})+K(4S_{1/2}) \rightarrow Na^*(3P_{3/2})+K(4S_{1/2})$ processes, *Z. Phys., D At. Mol. Clust.* 34 (1995) 163–170.
- [26] V. Horvatic, C. Vadla, M. Movre, K. Niemax, The collision cross sections for the fine-structure mixing of caesium 6P levels induced by collisions with potassium atoms, *Z. Phys., D At. Mol. Clust.* 36 (1996) 101–104.
- [27] T.L. Correll, V. Horvatic, N. Omenetto, C. Vadla, J.D. Winefordner, Quantum efficiency improvement of a cesium based resonance fluorescence detector by helium-induced collisional excitation energy transfer, *Spectrochim. Acta Part B* 60 (2005) 765–774.
- [28] C. Vadla, V. Horvatic, K. Niemax, Radiative transport and collisional transfer of excitation energy in Cs vapors mixed with Ar or He, *Spectrochim. Acta Part B* 58 (2003) 1235–1277.
- [29] A.C.G. Mitchell, M.W. Zemansky, *Resonance Radiation and Excited Atoms*, University Press, Cambridge, 1971.
- [30] A. Thorne, U. Litzén, S. Johanson, *Spectrophysics — Principles and Applications*, Springer Verlag, Berlin, 1999.
- [31] Z.J. Jabbour, J. Sagle, R.K. Namiotka, J. Huennekens, Measurement of the self-broadening rate coefficients of the cesium resonance lines, *J. Quant. Spectrosc. Radiat. Transfer* 54 (1995) 767–778.
- [32] A.N. Nesmeyanov, in: R. Gray (Ed.), *Vapor pressure of the chemical elements*, Elsevier, Amsterdam, 1963.
- [33] J.B. Taylor, I. Langmuir, Vapor pressure of caesium by the positive ion method, *Phys. Rev.* 51 (1937) 753–760.
- [34] W. Demtröder, *Laser Spectroscopy*, Springer Verlag, Berlin, 1995.
- [35] D.A. Smith, I.G. Huges, The role of hyperfine pumping in multilevel systems exhibiting saturated absorption, *Am. J. Phys.* 75 (2004) 631–637.
- [36] W. Hansen, The application of polarisation-influenced Thomas–Fermi ion models to alkali-atom transitions, *J. Phys. B: At., Mol. Opt. Phys.* 17 (1984) 4833–4850.
- [37] P.L. Smith, C. Heise, J.R. Esmond, R.L. Kurucz, Kurucz Atomic Line Database, <http://cfa-www.harvard.edu/amdata/ampdata/kurucz23/sekur.html>.
- [38] A.A. Radzig, B.M. Smirnov, *Reference data on atoms, Molecules and Ions*, Springer-Verlag, Berlin, 1985, pp. 97–105.
- [39] N.Ph. Georgiades, E.S. Polzik, H.J. Kimble, Two-photon spectroscopy of the $6S_{1/2} \rightarrow 6D_{5/2}$ transition of trapped atomic cesium, *Opt. Lett.* 19 (1994) 1474–1476.
- [40] T.L. Correll, V. Horvatic, N. Omenetto, J.D. Winefordner, C. Vadla, Experimental evaluation of the cross-sections for the $Cs(6D) \rightarrow Cs(7P_J)$ and $Cs(6D_{5/2}) \rightarrow Cs(6D_{3/2})$ collisional transfer processes induced by He and Ar, *Spectrochim. Acta Part B* 61 (2006) 623–633.
- [41] A.C. Tam, T. Yabuzaki, S.M. Curry, M. Hou, W. Happer, Inelastic cross sections in $Cs(n\ ^2D_J)+Cs(6\ ^2S_{1/2})$ collisions, *Phys. Rev., A* 17 (1978) 1862–1868.
- [42] P.W. Pace, J.B. Atkinson, Transfer of electronic excitation between $7^2P_{1/2}$ and $7^2P_{3/2}$ states of cesium induced by collisions with cesium atoms, *Can. J. Phys.* 52 (1974) 1641–1647.